From Proceeding of the 1999 ASME IMECE
Nashville, TN November 14-19. 1999

DSC-7B-2

Friction Identification for Haptic Display

Christopher Richard, Mark R. Cutkosky
Stanford University Center for Design Research
560 Panama Street
Stanford, CA, 94305-2232,USA
crichard@cdr.stanford.edu

Karon MacLean
Interval Reseach Corporation
1801 Page Mill Road
Palo Alto, CA 94304, USA

ABSTRACT

A method of identifying the friction of real devices for haptic display is presented. The method is suitable for identifying both the friction and inertia of a system simultaneously. This paper begins with a brief survey of common friction models and identification procedures. After the identification method is outlined, results are presented for experiments conducted to identify the friction and mass of an aluminum block sliding on sheets of brass, teflon, and rubber.

INTRODUCTION

One use of haptic interfaces is to imbue interaction with virtual models with the same sense of force, motion and texture offered by physical system dynamics. The challenge of creating realistic, high fidelity representations of physical devices or mechanisms has received much attention by haptics researchers and haptic system developers. Objects such as switches and springs, with impedance characteristics dominated by stiffness, inertia, and damping, have been successfully modeled and subsequently rendered with the same haptic interface. We seek to extend the realm of haptic identification and display to include objects with substantial friction. Friction is present at some level in all sliding objects and mechanisms with sliding parts. Knowledge of an environment's friction is essential to understanding and modelling the system dynamics. Nevertheless, because it is highly nonlinear, friction is rarely fully included in haptic renderings. Friction is often simplified and represented as a constant plus linear damping term, even when the details of the friction can be valuable for distinguishing among different materials.

The problem of identifying friction is complicated when the environment's inertia is also unknown. Unlike stiffness, which can be measured statically, friction identification involves dynamic measurements, which are invariably affected by mass and damping as well. It is possible to include damping in a general friction model, but inertial forces must be isolated. In some cases, it is possible to disassemble a mechanism or otherwise operate on it so that the mass can be evaluated independent of friction. In the most general case, however, the mass and friction must be estimated simultaneously.

The work presented here will illustrate a method for actively probing an object or device in the environment to create a haptic model of its friction characteristics and of its inertia. We begin by highlighting some of the previous work in system identification and friction measurement. Next we discuss some of the friction models that appear frequently in the literature. After selecting an appropriate friction model, we detail an algorithm for haptic friction identification. We conclude with a presentation of our results and a discussion of the algorithm's effectiveness.

PREVIOUS WORK

Environment and Device Identification

There are several examples of haptic interfaces used for system identification in the literature. Shulteis et al.[1996] demonstrated that a haptic system used for teleoperation can extract quantities such as an object's dimensions, weight and coefficient of friction. Dupont et al.[1997] showed that the same system can be used to identify the kinematic constraints of an object being manipulated. MacLean [1996] used a haptic interface equipped with a force sensor as a force probe to characterize the nonlinear stiffness properties of a momentary

switch. The characterization was done by first recording the force response of the switch over a range of displacements. Next, the nonlinear force versus displacement profile was divided into piecewise linear segments. The obtained stiffness model was then used to simulate the switch using the same interface that characterized it. Miller and Colgate [1998] used a wavelet network (a nonlinear system identification technique) to identify the impedance characteristic of a spring attached to a wall. The wavelet technique, like MacLean's method, uses force/displacement data collected from a real system. However, the wavelet analysis is done in the spatial frequency domain.

Friction Identification

Johnson and Lorenz [1992] present a novel method for identifying a system's friction by measuring state feedback errors. They begin by building a feed-forward controller that includes relevant dynamic properties of the system such as its mass and viscous damping. The controller does not include compensation for Coulomb friction. Once the feed-forward gains for inertia and viscous damping are properly tuned, the state feedback error signal will contain only errors caused by friction and other unmodeled effects. The unmodeled effects are then minimized with a signal processing technique called Synchronous Spatial Averaging, SSA. SSA averages velocity signals in the spatial velocity domain rather than in the time domain. Averaging in this manner filters noise signals that are uncorrelated to spatial velocity.

Kim et al.[1996] use a numerical optimization scheme to find the unknown parameters of their chosen friction model. Seeking to characterize the friction in an x-y plotter, the authors operate the system by applying a specified force input. The plotter displacement is then recorded. Starting with initial estimates for the friction model parameters, their optimization scheme adjusts the parameters until optimal values are found. The optimal set of parameters minimizes the square of the error between the recorded displacement and the displacement predicted by the model.

Armstrong-Helouvry [1991] used two main schemes to measure the friction present in robotic joints. In the first method, a known torque trajectory was applied to the system while the acceleration was recorded. Because the system's inertia was known, the friction could be calculated as the difference between the known input torque and the calculated inertial torque. The second method estimated static friction by measuring the minimum input torque necessary to initiate motion.

Kim et al.[1997] began by selecting an exponential friction model. They used least squares regression in the frequency domain and solved for the parameters of their model.

In each of these cases, the first step in friction identification was the selection of the model to be used. The second step was to determine the values for the parameters of the model.

FRICTION MODEL SELECTION

For an extensive survey of friction models, the reader is referred to Armstrong-Helouvry et al.[1994]. As previously mentioned, linear viscous damping is the most commonly utilized model of friction (Figure 1(a)). Unfortunately, viscous damping is rarely encountered. The next most common model of friction is credited to Coulomb. Coulomb's model states that the frictional force always opposes the velocity and its magnitude is constant when the velocity is non-zero. When the velocity is zero, the frictional force takes on whatever value is necessary, up to the static friction limit, to cancel the results of other applied forces so that the zero velocity condition is maintained (Figure 1(b)). Coulomb friction can be added to the viscous friction model as Figure 1(c) illustrates.

The phenomenon of "stiction" or "stick-slip" is modeled by allowing the static value of friction to be higher than the dynamic value (Figure 1(d)). Variations of this model include Karnopp's [1985] model where the static friction condition exists at non-zero velocity if the magnitude of the velocity is less than a small, predefined value (Figure 1(e)). The Stribeck effect says that the value of the friction force decreases as velocity increases in the low velocity regions of the friction curve (Figure 1(f)).

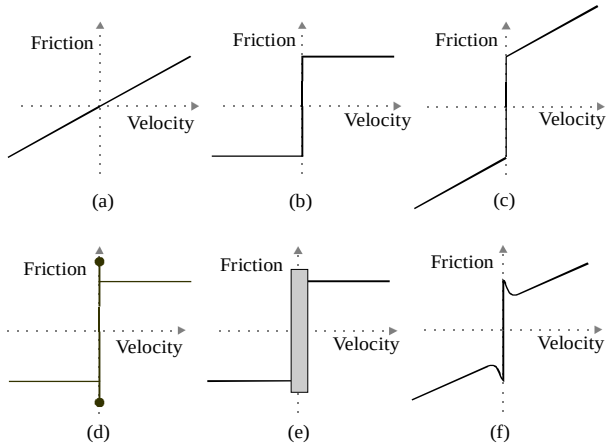

Figure 1. Friction Models: (a) viscous damping; (b) Coulomb model; (c) Coulomb and viscous; (d) "stiction"; (e) Karnopp's model; (f) the Stribeck effect.

Armstrong et al.[1994] present a seven-parameter integrated friction model that encompasses all of the phenomena discussed above as well as additional effects such as frictional memory and rising static friction with dwell time.

Dahl, [1976] presents a model that describes friction primarily as a function of displacement. Dahl's model is a differential equation that gives the change in friction with respect to position. The model is based on the physical phenomenon of pre-sliding displacement. It is able to capture the hysteretic behavior often observed in friction. Hayward and

Armstrong, [1999], have successfully used a Dahl-based model to simulate friction on a haptic device.

Most dry friction models contain a hard nonlinearity at zero velocity represented with the signum function (*sgn*). There are, however, a collection of continuous friction models that model the steep transitional portion of the friction curve using exponential functions. Majd et al.[1995] provide one such model. The model is continuous in velocity and can include the Stribeck effect.

For haptic friction identification, we use a modified version of Karnopp's friction model [Karnopp 1985] (See Figure 2). The model includes both Coulomb and viscous friction and allows for asymmetric friction values for positive and negative velocities. It is expressed as:

$$F_{\text{friction}}(\dot{x}, F_a) = \begin{cases} C_n \text{sgn}(\dot{x}) + b_n \dot{x} & \text{for } \dot{x} < -\Delta v \\ max(D_n, F_a) & \text{for } -\Delta v < \dot{x} < 0 \\ min(D_p, F_a) & \text{for } 0 < \dot{x} < \Delta v \\ C_p \text{sgn}(\dot{x}) + b_p \dot{x} & \text{for } \dot{x} > \Delta v \end{cases}$$

where

C_p and C_n are the positive and negative values of the dynamic friction;
b_p and b_n are the positive and negative values of the viscous friction;

$\dot{x}$ is the relative velocity between the mating surfaces;
D_p and D_n are the positive and negative values of the static friction;
Δv is the value below which the velocity is considered to be zero, and;
F_a is the sum of non-frictional forces being applied to the system.

Although this model cannot replicate subtle friction features such as the Stribeck effect, it does model the basic stick-slip property. By allowing the friction force to be asymmetric, this model better matches data observed here and in other friction identification papers [Armstrong 1991,Johnson and Lorenz 1992]

EXPERIMENTAL APPARATUS

A one degree of freedom linear motion haptic interface was constructed in order to conduct friction identification experiments (See Figure 2). The setup includes a low friction, low inertia, dc motor (Maxon RE025-055) as the actuator. A 2048 line quadrature encoder is used for position sensing. Velocity is estimated with the aid of an I/O Card from Immersion Inc. This card calculates velocity values by measuring the time between encoder pulses rather than counting the number of encoder pulses that occur during a specified time.

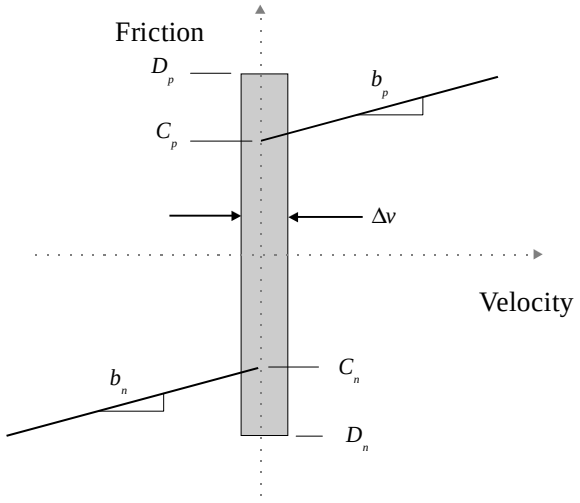

Figure 2. Parameters of the modified Karnopp model

Rotary motion from the motor is converted to linear motion/ force using a low friction linear stage and a transmission consisting of a steel cable wound several times around the motor pulley. A 10 lb. (44.8 N) capacity load cell (Sensotec31/1426-04) gives force measurements and a +/-50g accelerometer (Sensotec 60-3629-02) provides acceleration measurements. Estimates of key characteristics, including noise levels, of the apparatus are listed in Table 3 in the Appendix.

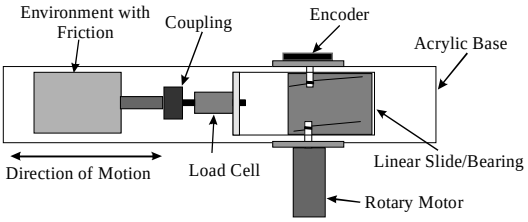

Figure 3. Schematic (top view) of the experimental apparatus.

The force sensor for the apparatus is located downstream of the motor and slide inertia so that it only measures the force applied to the object or system under test. The system being tested and the experimental apparatus are connected by a coupling that is compliant in the radial direction but stiff in the axial direction. The apparatus was used to identify sliding friction between an aluminum block and sheets of brass, teflon and rubber.

IDENTIFICATION PROCEDURE

The procedure for friction identification can be summarized as follows:

- Model the force/motion interaction of the system

- Move system over a range of velocities of interest
- Record force/motion variables included in the model
- Solve for unknown parameters of the system model

These steps are detailed below.

Modeling the force/motion interaction

For our experimental system the force/motion interaction can be described as

$$F_{\text{applied}} = m\ddot{x} + F_{friction} + F_{other} \quad (1)$$

where

$F_{applied}$ is the force applied to the aluminum block;
m is the mass of the aluminum block;
$\ddot{x}$ is the acceleration of the aluminum block;
$F_{friction}$ is the modified friction model described by Eq. (1), and;
F_{other} includes any effects not included in the inertia term or in the friction model.

Terms in F_{other} can include things such as off-axis force sensor loading, forces caused by elastic deformations, and an inertial force out of line with the primary direction of motion.

Move system over range of velocities of interest

For each friction measurement experiment the aluminum block was connected to the apparatus and the apparatus was commanded to move with a periodic trajectory. Various periodic trajectories having frequencies ranging between of 0.5-3 Hz were explored. The sample trajectories presented here are sinusoids with a frequency of 2 Hz and an amplitude of 0.01 meters. The system was driven using a proportional-derivative or PD controller. The PD gains were tuned before the apparatus was connected to a system with friction. They were empirically set to the highest values that gave smooth sinusoidal responses without friction. For additional smoothing, the command output was digitally filtered with a second order low-pass filter with a cut-off frequency of 100Hz. The frequency and amplitude of the command trajectory were selected to stay within the 0.030 meter range of motion of the interface and to match the approximate range of motions that humans use when sliding their fingertips in an exploratory fashion. The sample rate for motion commands and data collection was 1 kHz.

Record force/motion variables included in the model

The system was allowed to warm-up for 10 seconds prior to collecting data for each experiment. During the warm-up, the aluminum block was moved with the same sinusoidal trajectory that was used during data collection. The warm-up served two functions. First, it eliminated the phenomenon of rising static friction because the system was not allowed to dwell at zero velocity for a significant period. Second, it allowed the motion of the system to reach steady state. After the 10 second warm-up was complete, the force applied to the aluminum block was recorded, along with the block's position, velocity and acceleration. Data were collected for 2 seconds, corresponding to four cycles and seven velocity reversals. Figure 3 shows typical velocity, acceleration and force data.

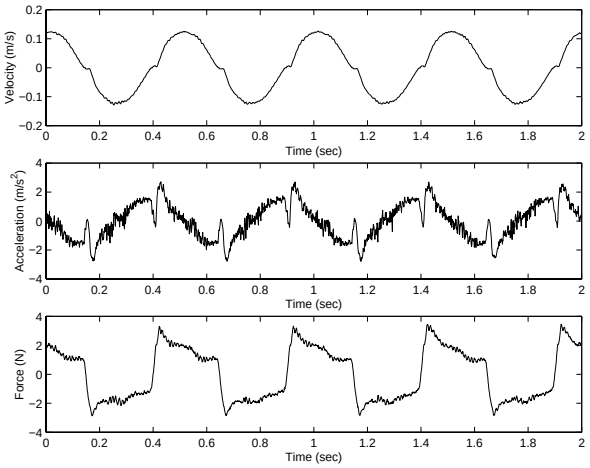

Figure 4. Typical velocity, acceleration, and force data.

Due to the digital nature of the encoder, position and velocity estimates were obtained with a relatively small measurement error. Force and acceleration estimates, however, had larger uncertainties arising primarily from noise introduced in signal amplification and analog to digital conversion (See Table 1).

Table 1: Standard Deviations of the Measurement Errors

Measurement Error	Standard Deviation	Units
position	5.76×10^{-5}	meters
velocity	3.18 x 10-3	meters/second
acceleration	0.2379	meters/second^2
force	0.062	Newtons

The uncertainty estimates are the standard deviations of the difference between the measured trajectories and ideal trajectories. These are conservative estimates since a portion of the difference can be attributed to errors in the control.

To help reduce the errors caused by the drift and temperature sensitivity in the accelerometer, the acceleration signal was scaled and offset for each experimental run. The scale factor and offset were selected to minimize the difference between the accelerometer measurement and a differentiated velocity signal. The differentiated velocity signal was obtained by four-point central differencing. The resulting adjusted acceleration signal contains less noise than the differentiated velocity signal and is more accurate than the original accelerometer measurement.

Solve for unknown parameters of the system model

With our modeling and data collection complete we can estimate the parameters of our friction model. By expressing the parameters of our model as linear coefficients of our inputs the parameters can be estimated using Least Square Regression (LS).

As a first step in expressing the model parameters in a linear fashion, we separate the data into two bins. One bin contains data for velocities of magnitude less than Δv. The second bin holds the remaining data. Δv is selected as the smallest velocity range that fully encompasses the transition from static to dynamic friction. After the data points corresponding to low velocities are removed, the recorded velocity vector is split into two new velocity vectors. The velocity vector vel_p is equal to the original vector *vel* except that negative velocity values are replaced with zeros. The velocity vector vel_n contains the negative portion of the original velocity vector and has zeros where there are positive values in *vel* (See Figure 4).

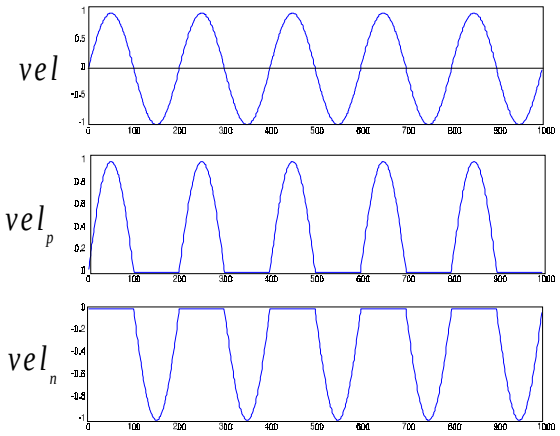

Figure 5. Example of how velocity is split into positive and negative components.

Now, the measured force can be expressed as the sum of the inertia force, and the friction by

$$\boldsymbol{F_m} = m\mathbf{a} + C_p \mathrm{sgn}(\mathbf{vel_p}) + b_p \mathbf{vel_p} + C_n \mathrm{sgn}(\mathbf{vel_n}) + b_n \mathbf{vel_n} + \varepsilon \quad (2)$$

or, in matrix form as

$$\begin{bmatrix} F_{m1} \\ \dots \\ F_{mN} \end{bmatrix} = \begin{bmatrix} a_1 & \mathrm{sgn}(vel_{p1}) & vel_{p1} & \mathrm{sgn}(vel_{n1}) & vel_{n1} \\ \dots & \dots & \dots & \dots & \dots \\ a_N & \mathrm{sgn}(vel_{pN}) & vel_{pN} & \mathrm{sgn}(vel_{nN}) & vel_{n1N} \end{bmatrix} \begin{bmatrix} m \\ C_p \\ b_p \\ C_n \\ b_n \end{bmatrix} + \begin{bmatrix} \varepsilon_1 \\ \dots \\ \varepsilon_N \end{bmatrix} \quad (3)$$

$$\boldsymbol{F_m} = \boldsymbol{X}\beta + \varepsilon \quad (4)$$

where

$\boldsymbol{F_m}$ is the measured force;
a is the measured acceleration and;
ε is the measurement error.

The LS estimate for β has been shown to be

$$\hat{\beta} = (\boldsymbol{X}^T\boldsymbol{X})^{-1}(\boldsymbol{X}^T\boldsymbol{F}_m) \quad (5)$$

Implicit in this estimate for β is the assumption that the variables in $\boldsymbol{X}$, and *vel* in our case, are free of measurement error. Fuller[1987] shows that β's estimated using Eq. (6) will contain a bias if measurement error is present. Given the fact that measurement errors exist in both *a* and *vel*, we consider an alternate estimator for β. Fuller goes on to present several alternate estimators that account for errors in the input variables and provide unbiased estimates of β. Assuming that the errors in each of our measured variables are independent of each other, our alternate estimate for β is

$$\tilde{\beta} = (N^{-1}\boldsymbol{X}^T\boldsymbol{X} - \ddot{S}_{uu})^{-1}(N^{-1}\boldsymbol{X}^T\boldsymbol{F}_m) \quad (6)$$

where

N is the number of samples;

$\ddot{S}_{uu} = \mathrm{diag}(s_{\delta a}, 0, s_{\delta vel}, 0, s_{\delta vel})$;

$s_{\delta a}$ is the estimated variance of the acceleration, and;

$s_{\delta vel}$ is the estimated variance of the velocity.

RESULTS

Here we present results obtained by using the method outlined in the previous section to identify the friction and mass of an aluminum block sliding on brass, teflon and rubber. The mass of the block was presumed unknown for each experiment; however, for verification purposes the block was weighed and found to be 0.419 kg. Figures 6(a), 7(a) and 8(a) show typical raw force data plotted against velocity for our three material combinations. The effects of some stick-slip vibration are evident in the plots. Figures 6(b), 7(b), and 8(b) show the raw force adjusted for the estimated mass. The solid lines in Figures 6(b), 7(b), and 8(b) represent the predicted friction for each case using the parameters in Eq. (3). The rectangular box shows Δv, D_n and D_p from Eq. (1).

Table 2 lists estimates of the friction model parameters and their standard deviations. For information about calculating the standard deviations of the parameter estimates obtained by Eq. (7), the reader is referred to Fuller [1987]. Two experimental runs are presented for each material combination to give a sense of the friction model parameter repeatability from setup to setup. The use of Eq. (6) rather than Eq. (5) had the most profound effect on the mass estimates. Mass estimates are 3.8% larger for brass and rubber and 5% larger for teflon.

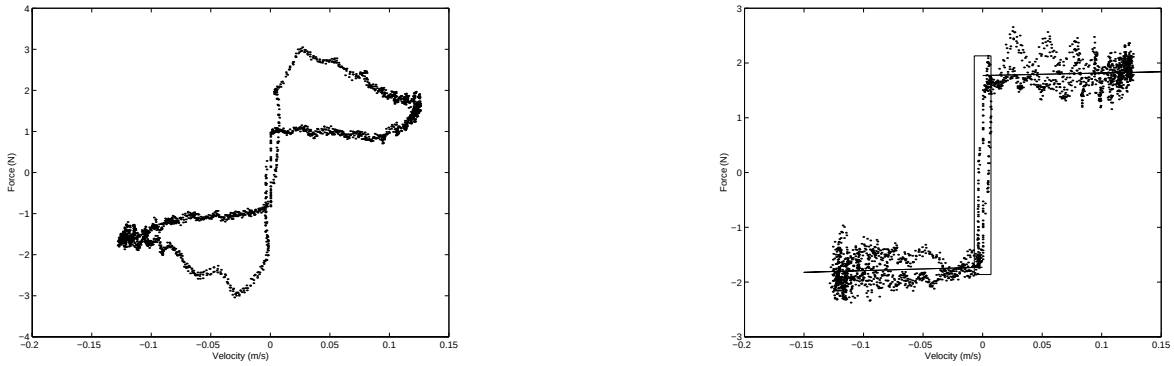

(a) **(b)**

Figure 6. (a) Measured force versus velocity for aluminum on brass (four motion cycles). (b) Measured force adjusted for mass and model estimated friction for aluminum on brass.

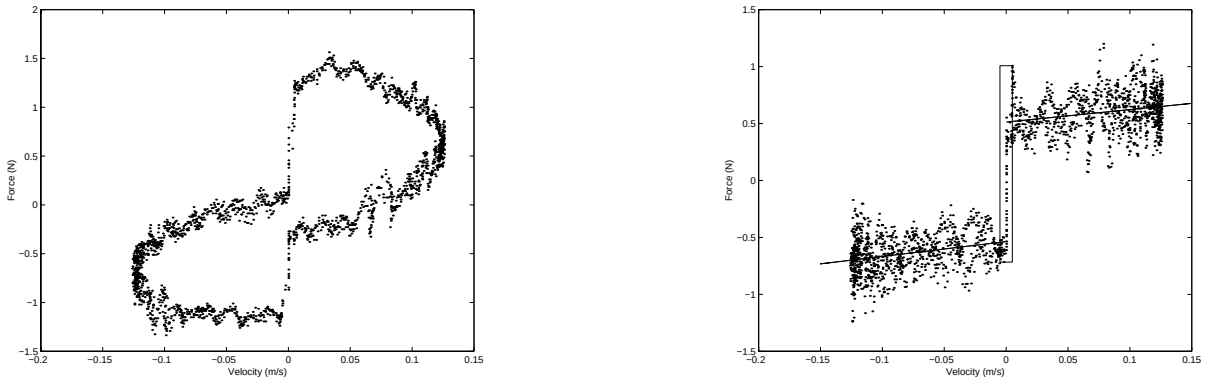

(a) **(b)**

Figure 7. (a) Measured force versus velocity for aluminum on teflon (four motion cycles). (b) Measured force adjusted for mass and model estimated friction for aluminum on teflon.

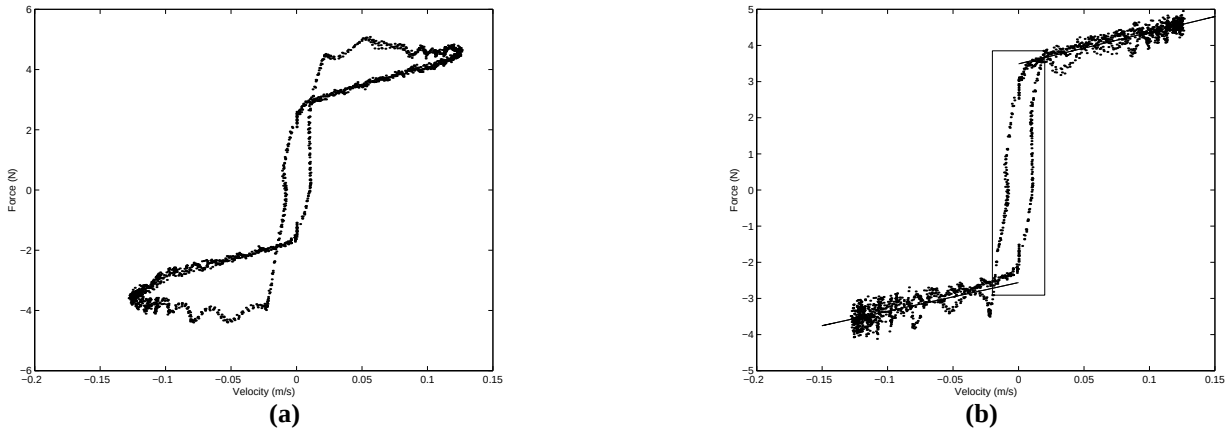

(a) **(b)**

Figure 8. (a) Measured force versus velocity for aluminum on rubber (four motion cycles). (b) Measured force adjusted for mass and model estimated friction for aluminum on rubber.

Table 2: Friction estimates for aluminum sliding on brass, teflon and rubber using Fuller's method (Eq. (6)). The parameters correspond to the modified version of Karnopp's model (Eq. (1)).

	Brass1		Teflon1		Rubber1	
Parameter	Estimate	Std Dev	Estimate	Std Dev	Estimate	Std Dev
m	0.4033	0.0051	0.4436	0.0038	0.3886	0.0045
Cp	1.7714	0.023	0.513	0.0136	3.4901	0.0334
bp	0.457	0.248	1.0957	0.1519	8.7338	0.3621
Cn	1.729	0.0229	0.5365	0.0133	2.5611	0.0298
bn	0.6196	0.2504	1.3038	0.15	7.9521	0.3225
Dp	2.1302		1.0078		3.8513	
Dn	-1.8623		-0.7167		-2.9099	
Δv	0.007		0.005		0.02	
	Brass2		Teflon2		Rubber2	
Parameter	Estimate	Std Dev	Estimate	Std Dev	Estimate	Std Dev
m	0.4117	0.0039	0.4555	0.0037	0.3737	0.0047
Cp	1.6814	0.0173	0.4808	0.0132	3.7244	0.0353
bp	-1.5778	0.1884	1.6554	0.1476	9.6733	0.3853
Cn	1.6384	0.0174	0.5233	0.0127	2.7269	0.0296
bn	-0.618	0.1894	1.5635	0.1434	8.0322	0.3213
Dp	2.0842		0.9319		4.0179	
Dn	-1.7328		-0.6553		-2.7733	
Δv	0.007		0.005		0.02	

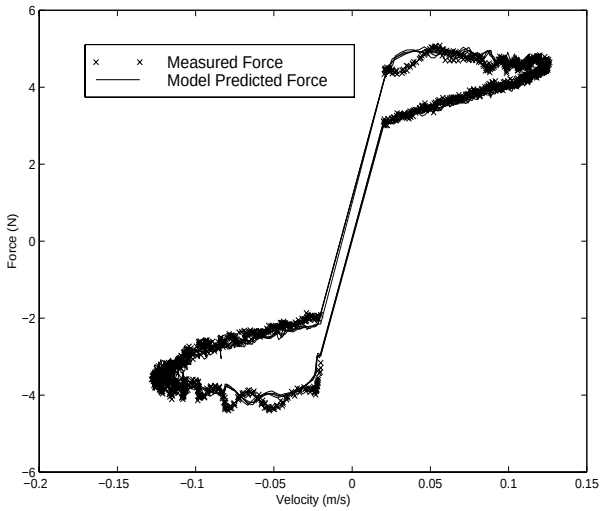

FIGURE 9. Typical measured force and model predicted force versus velocity (aluminum on rubber) over four cycles of motion.

The goodness of the model's fit can be seen in Figure 9, which is a plot of the measured force and the model predicted force for aluminum on rubber. Both measured force and model predicted force are plotted against velocity.

The reader will note that second and third columns and the fourth and fifth columns in the matrix $\boldsymbol{X}$, defined in Eq.(3) and Eq. (4), columns 2 and 3 and 4 and 5 are related through signum function. For velocity values that are strictly positive, the linear correlation between vel_p and sgn(vel_p) is undefined. Similarly, when the velocity is strictly negative, there is no linear correlation between vel_n and sgn(vel_n). However, because both vel_p and vel_n contain zeros, there is a quantifiable linear correlation between columns 2 and 3 and between columns 4 and 5. The relationship between the independent variables causes the matrix $\boldsymbol{X}$ to exhibit some multicollinearity. Multicollinearity leads to a poorly conditioned $\boldsymbol{X}^T\boldsymbol{X}$ matrix, and subsequently poor parameter estimates. For the data presented in this paper the $\boldsymbol{X}^T\boldsymbol{X}$ matrices for all materials have condition numbers on the order of 10^{-4}. Matrices with condition numbers on this order are readily invertible with numerical software packages such as MATLAB®.

CONCLUSIONS AND DISCUSSION

This paper has presented a method for using a haptic interface to estimate the friction and inertia of a real device or system. Sample results were presented for the friction force and mass estimate of an aluminum block sliding on brass, teflon and rubber. Unlike other friction identification techniques, it does not require the experimenter to carefully tune a feed-forward controller. Furthermore, it is not susceptible to the convergence problems of some numerically based techniques. Lastly, it does not fit an complex model to the experimental data.

As is often the case with control or identification strategies, accurate measurements of velocity and acceleration are the key to accurate friction and mass estimates using the method presented here. Much of the spread in the data adjusted for mass (Figures 6(b), 7(b), and 8(b)) can be attributed to noise in the accelerometer. The effect appears to be less drastic for aluminum on rubber, but this is due to the larger magnitude of the friction force for rubber. The larger the relative magnitudes of the mass and viscous damping for the system being identified, the more acceleration and velocity errors will affect one's estimate. In general, the effect of acceleration and velocity errors will be less profound on estimates of the dynamic friction parameters C_p and C_n.

In addition to measurement accuracy, the selection of the excitation trajectory is important. While it seems that virtually any input trajectory should suffice for friction and mass estimates, the best results were obtained when smooth sinusoidal closed-loop position trajectories were used. Open-loop force input trajectories did not provide good results. Finding the appropriate amplitude and frequency for an open-loop force input proved to be difficult. If the input force amplitude was made too small, the system would sit at rest, unable to overcome static friction. If the input amplitude was slightly larger, the system would crash into the hard stops delimiting its range of motion. Even if an appropriate open loop force trajectory was found for a given environment, that same trajectory would in all likelihood be inappropriate for a system with different inertia or friction properties.

The observed asymmetry in the friction data is included in the friction model. Because the force sensor is located between the haptic device, and the system with friction, effects like cable drag, D/A calibration offsets, and motor amplifier offsets should not result in asymmetric friction identification. Asymmetry in the force sensor, or in the force sensors amplifier can however lead to an asymmetric response. For this reason, great care should be taken when calibrating the force sensor.

Our selection of a modified version of Karnopp's friction appears to be a good choice for the range of materials presented here. The model allows for reasonable estimates of static and dynamic friction as well as viscous damping terms. It should be noted, however, that Karnopp's model is not necessarily the best representation of friction from a tribological point of view. Models that are based on the interaction of microscopic surface asperities, or on pre-sliding displacement are better able to capture subtle features of friction.

The hysteresis that is evident in Figures 6(b) and 9(b) is most likely due surface elasticity and/or some compliance in the system. This elasticity is, strictly speaking, not part of the friction, and therefore is not included in the model. The true test of the model's adequacy will come from psychophysical user testing.

ACKNOWLEDGEMENTS

Funding for this project was provided by Interval Research Corporation. In addition, Dr. Herb Rauch is gratefully acknowledged for his insight and advice.

REFERENCES

Armstrong-Helouvry, B., *Control of Machines with Friction*, Kluwer Academic Publishers, Norwell, MA. 1991.

Armstrong-Helvouvry, B., P. DuPont and C. Canudas De Wit, "Survey of Models, Analysis Tools and Compensation Methods for the Control of Machines with Friction," Automatica, Vol. 30, no. 7, pp. 1083-1138, 1994.

Dahl, P. R., "Solid Friction Damping of Mechanical Vibrations," AIAA Journal, v. 14, n. 12, pp. 1675-1682, 1976.

Dupont, P. E., T. M. Schulteis, and R. D. Howe, "Experimental identification of kinematic constraints," Proceedings of the 1997 IEEE International Conference on Robotics and Automation, ICRA. Part 3 (of 4), Albuquerque, NM, USA.Piscataway, NJ, p 2677-2682.

Fuller, W., *Measurement Error Models*, John Wiley and Sons, New York, 1987.

Hayward, V., B. Armstrong, "A new computational model of friction applied to haptic rendering." Preprints of ISER'99 (6th Int. Symp. on Experimental Robotics), Sydney, Australia, March 1999

Johnson, C. T., and R. D. Lorenz, "Experimental Identification of Friction and Its Compensation in Precise, Position Controlled Mechanism," IEEE Transaction on Industrial Applications, Vol. 28, no. 6 (November/December), Piscataway, NJ, pp. 1392-1398, 1992.

Karnopp D.,"Computer simulation of stick-slip friction in mechanical dynamic systems," ASME Journal of dynamic Systems, Measurement and Control, Vol. 107, pp. 100-103, 1985.

Kim, J.-H., H.-K. Chae, J.-Y. Jeon, and S.-W. Lee, "Identification and Control of Systems with Friction Using Accelerated Evolutionary Programming," IEEE Control Systems, August 1996, pp. 38-47, 1996.

Kim S. J., I.-J. Ha, J. H. Kang, C. H. Kim, S. G. Lim, "A New Parameter Identification Method for Mechanical Systems with Friction," Proceedings of the 1997 23rd Annual International Conference on Industrial Electronics, Control, and Instrumentation, IECON. New Orleans, LA, Vol. 1, p 322-327, 1997.

MacLean, K.,"The 'Haptic Camera': A technique for Characterizing and Playing Back Haptic Properties of Real Environments," Proceeding of ASME Dynamic Systems and Control Division, DSC Vol. 58, New York, NY, pp. 459-467, 1996.

Majd, V. J. and M A. Simaan, "A Continuous Friction Model for Servo Systems with Stiction," Proceedings of the 1995 IEEE Conference on Control Applications, Piscataway, NJ, pp. 296-301, 1995.

Miller B. E. and J. E. Colgate, "Using a Wavelet Network to Characterize Real Environment for Haptic Display," Proceedings of the ASME Dynamic Systems and Control Division, DSC Vol. 64, New York, NY, pp. 257-264, 1998.

Schulteis, T., P DuPont, P. Millman and R. Howe, "Automatic identification of remote environments," Proceedings of the ASME Dynamic Systems and Control Division, DSC Vol. 58, New York, NY, pp. 451-458, 1996.

APPENDIX

Table 3: Experimental Apparatus Parameters

System Equivalent Inertia (motor and slide)	0.692 kg
Force output to commanded voltage	23.315 N/V
Maximum Force (continuous)	9.48 N
Range of Motion	3.2 cm
Position Resolution	2.57×10^{-6} m
Voltage output to measured force	8.896 N/V
Static Friction (motor and slide)	
Forward Motion	1.04 N
Reverse Motion	0.69 N